Conformations of Dimethylhydrogen Phosphonate (DMHP): A Matrix Isolation Infrared and ab Initio Study

K. Sundararajan* and K. Sankaran

Materials Chemistry Division, Indira Gandhi Centre for Atomic Research, Kalpakkam 603 102, India

Received: January 22, 2008; Revised Manuscript Received: March 27, 2008

The infrared spectra of dimethylhydrogen phosphonate (DMHP) isolated in nitrogen, argon and krypton matrices using an effusive source at 298 and 373 K have been recorded. Experiments were also performed using a supersonic jet source to look for conformational cooling in the expansion process. As a result of these experiments, infrared spectral characteristics of the ground and higher energy conformers of the DMHP have been identified for the first time. The structures of DMHP were optimized at the hybrid B3LYP and Hartree fock (HF) levels of theory using the 6-31++G** basis sets. Computationally, four minima were obtained corresponding to DMHP conformers with $G^{\pm}G^{\mp}$, $G^{-}G^{-}$, TG^{+} and TG^{-} structures in the order of increasing energy. Frequency calculations were done to confirm that the structures were indeed minima on the potential energy surface (PES). The computed frequencies corroborated well with the experimental matrix isolation infrared frequencies leading to definite assignments of the infrared features of DMHP, for the $G^{\pm}G^{\mp}$ and TG^{+} conformers. At B3LYP/6-31++G** level, the energy difference between the $G^{\pm}G^{\mp}$ and $G^{-}G^{-}$ conformer was 1.53 kcal/mol, and that between $G^{\pm}G^{\mp}$ and TG^{+}, $G^{\pm}G^{\mp}$ and TG^{-} were 1.65 and 1.95 kcal/mol. Transition-state calculations were also carried out at B3LYP/6-31++G** level connecting the $G^{\pm}G^{\mp}$ to $G^{-}G^{-}$, TG^{+} and TG^{-} conformers. Computations indicated that the conformer interconversion between $G^{-}G^{-} \rightarrow G^{\pm}G^{\mp}$ is barrierless, whereas the barriers for $TG^{+} \rightarrow G^{\pm}G^{\mp}$ and $TG^{-} \rightarrow G^{\pm}G^{\mp}$ are 1.47 and 0.88 kcal/mol, respectively.

1. Introduction

Organic phosphonates are widely used as plasticizers, flame retardants and lubricants. They also play an important role in solvent extraction processes and pesticides in agriculture.[1,2] Simple alkyl phosphonates are relatively nontoxic and they are used as model compounds to mimic the properties of organophosphorus compounds in chemical research. Ewig and Van Wazer[3] arrived at three stable conformations of dimethylhydrogen phosphonate (DMHP) at STO-3G* basis set. When the calculations were performed using the 4-31G*//STO-3G* basis set, it predicted a different ordering by relative energy when compared with the STO-3G*; the 4-31G* basis yielded a set of relative energies that correlated well with their dipole moment. Ab initio computations on DMHP by Georgiev et al.[4] using HF/6-31+G* basis arrived at five possible conformations. With exception of one structure, all other structures corresponded to stable conformers. Barnes et al.[5] studied the conformations of dimethylmethyl phosphonate (DMMP) in liquid phase, gas phase, argon, nitrogen and carbon monoxide matrices. From these results they identified the existence of three conformers for DMMP and concluded that, depending upon the polarity of the matrix used, the conformer distribution varied during the deposition process. They did not observe any conformer interconversion on annealing the matrix at 35 K, clearly showing the conformer distribution is frozen once the matrix reaches low enough temperature. Neimark et al.[6] proposed a simple united-atom molecular model to study the conformations of DMMP. This model reproduced accurately the ab initio computations on the conformations of DMMP in vacuum and the experimental data on the physical properties of pure DMMP liquid. They have also used molecular dynamics simulations to explore the thermodynamic properties and molecular structure of aqueous solutions of DMMP. Katcyuba et al.[7] studied the conformations of dialkyl phosphites $(RO)_2P(O)H$ (R = C_2H_5, *n*-C_3H_7, *i*-C_3H_7, *n*-C_4H_{10} and *i*-C_4H_9). Vibrational spectra of liquid dialkyl phosphites showed broad features whereas the same liquid when cooled down to 170 K showed several crystal modifications and they have attributed this to each crystal consisting of different conformers of dialkyl phosphites. They could identify these conformers in the ν_{P-H} stretching frequency of dialkyl phosphites. Pieters et al.[8] studied the conformations of phosphinates $X_2PO(OCH_3)$, where X = F, Cl, or CH_3. In these experiments they did not observe any conformer distribution trapped in different matrices. In our laboratory we have studied the conformations of organophosphorus compounds such as trimethyl phosphate (TMP)[9,10] and triethyl phosphate (TEP)[11] using matrix isolation infrared technique and ab initio computations. In the present work we have studied the conformations of dimethylhydrogen phosphonate (DMHP).

2. Experimental Section

Matrix isolation experiments were carried out using a Leybold AG closed cycle compressor cooled cryostat, RD 210. The details of the vacuum system and cryogenics are described elsewhere.[12] Dimethylhydrogen phosphonate (DMHP) was prepared by slowly adding phosphorus trichloride (Merck) (0.33 mol) to methanol (HPLC grade) (1 mol) with constant stirring under an argon atmosphere over a period of 30−45 min at −10 °C.[13] The stirring was continued for half an hour more after the complete addition of PCl_3 to remove the liberated HCl. Chloromethane and unreacted methanol were removed from the sample by rotary pump. The DMHP was finally vacuum distilled and characterized by infrared and ^{31}P NMR techniques.

* To whom correspondence should be addressed. E-mail: sundar@igcar.gov.in.

10.1021/jp800604y CCC: $40.75
Published on Web 06/06/2008

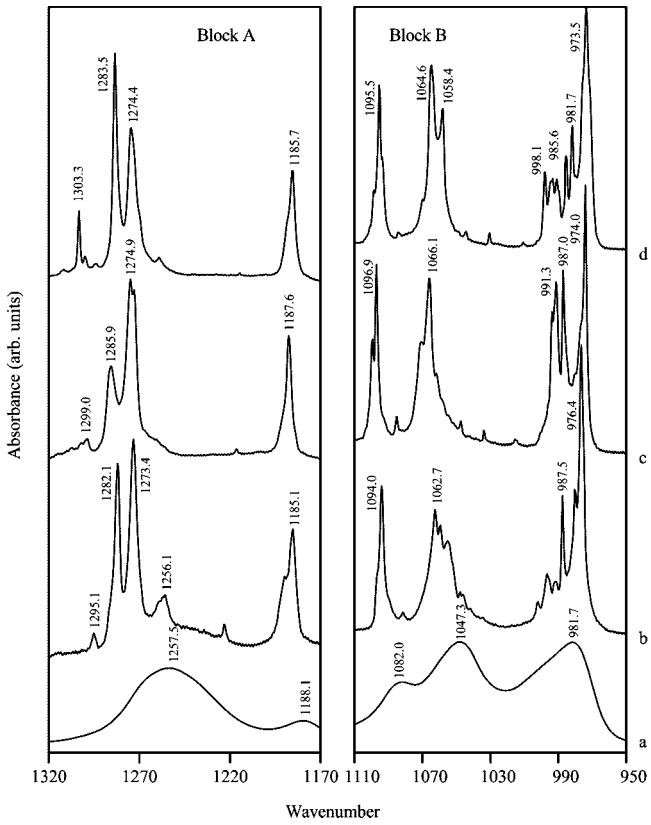

Figure 1. Infrared spectra of DMHP spanning the regions 1320−1170 cm^{-1} (block A) and 1110−950 cm^{-1} (block B): (a) liquid DMHP (at room temperature); matrix isolation infrared spectrum of DMHP in (b) nitrogen matrix, (c) argon matrix and (d) krypton matrix. Spectra shown are in as-deposited matrices.

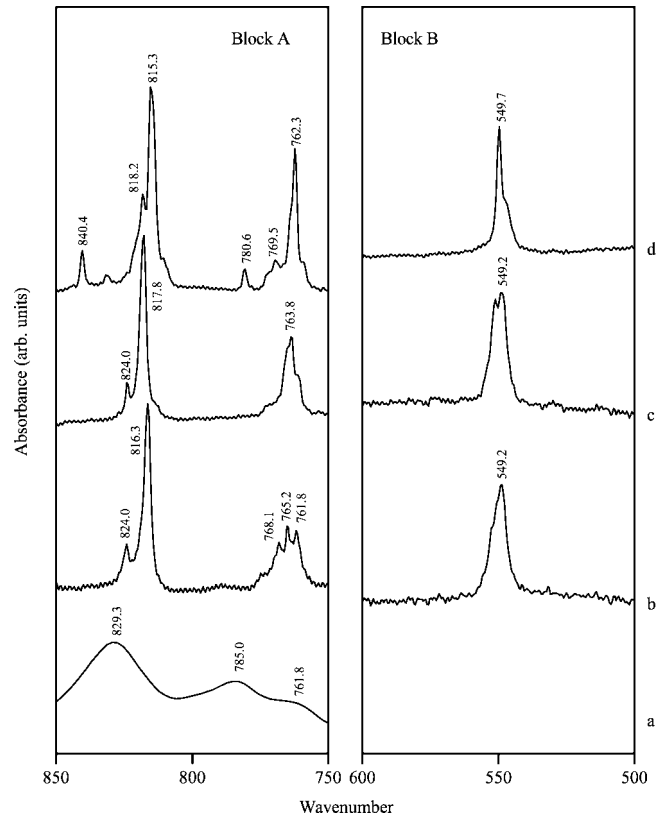

Figure 2. Infrared spectra of DMHP spanning the regions 850−750 cm^{-1} (block A) and 600−500 cm^{-1} (block B): (a) liquid DMHP (at room temperature); matrix isolation infrared spectrum of DMHP in (b) nitrogen matrix, (c) argon matrix and (d) krypton matrix. Spectra shown are in as-deposited matrices.

DMHP and the matrix gas ($Ar/N_2/Kr$) were mixed at a typical ratio of 1:1000. High-purity argon, nitrogen (Grade INOX-I, Ultrapure) and krypton (Bhuruka Gases Ltd., 99.997%) were used as matrix gases. The gas mixture was then allowed to stream out of a single-jet effusive nozzle and deposited onto a cold KBr window maintained at temperatures below ∼15 K. The deposition was carried out at a rate of ∼3 mmol h^{-1}, and a typical deposition lasted for ∼45 min. Spectra were recorded using a BOMEM MB100 FTIR spectrometer with a spectral resolution of 1 cm^{-1} and are referred to as "as deposited spectra". After the spectrum was recorded, the matrix was warmed to 25, 30 and 35 K depending upon the matrix gas used for the experiment, kept at this temperature for ∼15 min, and then recooled to 15 K. The spectra of the matrix thus annealed were then recorded. Experiments were also performed by maintaining the effusive source at different nozzle temperatures, viz. 298 (room temperature), 373 and 435 K. In the heated nozzle experiments, the nozzle was heated to a length of 35 mm, just prior to the exit of the gas mixture into the vacuum. We also performed experiments using a supersonic jet nozzle to deposit the sample mixture. For this purpose, a pulsed supersonic nozzle of 0.5 mm diameter (Parker Hannifin Corp.) was used, with the stagnant pressure of typically 1.3 atm. The pulsed valve was operated with a pulse width of 2 ms at a repetition rate of 0.3 Hz in all the experiments. At this deposition rate, the temperature of the cryotip did not rise. The spectrum of liquid DMHP, at room temperature, was also recorded using ZnSe window for comparison with the matrix-isolated spectra.

3. Computational Method

Ab initio molecular orbital calculations were performed using the Gaussian 94W program on an Intel Pentium (R) IV machine.[14] Geometry optimizations were done at both the HF and B3LYP levels using 6-31++G** basis set, without imposing any constraints during the optimization process. Vibrational frequency calculations were done at both HF and B3LYP levels using 6-31++G** basis set. The computed frequencies were scaled to bring them into agreement with experimental frequencies. To arrive at the scaling factor, the experimentally observed strongest feature in N_2 matrix (976.4 cm^{-1}) that could be assigned to the ground-state conformer was correlated with that of the strongest computed feature for the same conformer. The scaling factor of 1.005 was obtained at B3LYP/6-31++G** level. This scaling factor was used to scale all other vibrational frequencies. Vibrational frequency calculations also helped in ascertaining that the computed conformations did indeed correspond to a minimum on the potential energy surface. Zero point energies were also calculated. The transition-state structures connecting the ground-state and the higher energy conformers were also computed at B3LYP/6-31++G** level, from which the barrier to conformer interconversion were obtained.

4. Results and Discussion

Experimental Details. Figures 1 and 2 (block A and B) show the infrared (IR) spectra of DMHP deposited using an effusive nozzle source in nitrogen, argon and krypton matrices spanning the region 1320−1170, 1110−950, 850−750 and 600−500 cm^{-1}. These regions correspond to the P═O stretching, P−(O−C)

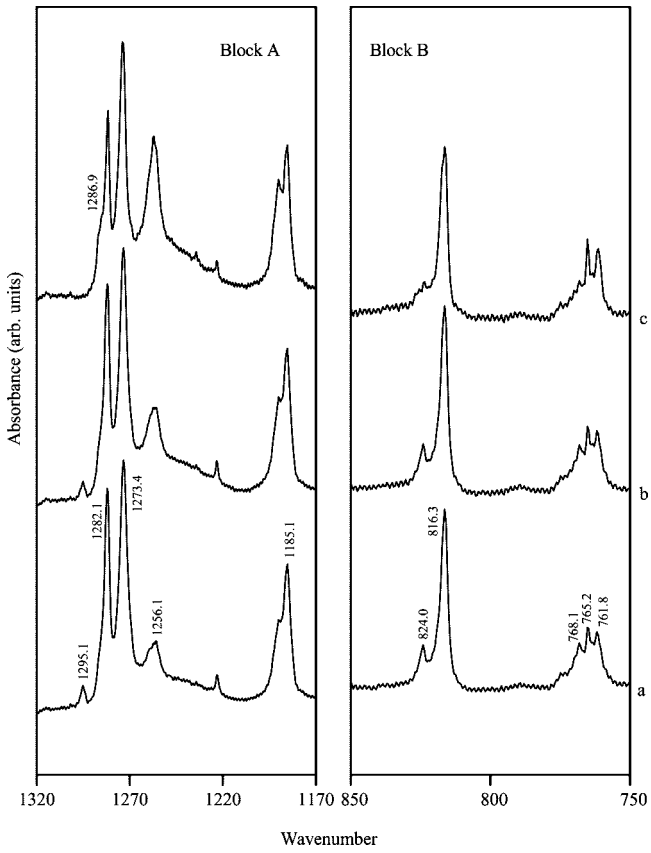

Figure 3. Matrix isolation infrared spectra of DMHP at different annealing temperatures in nitrogen matrix spanning the regions 1320−1170 cm^{-1} (block A) and 850−750 cm^{-1} (block B): (a) 12 K; (b) 25 K; (c) 30 K.

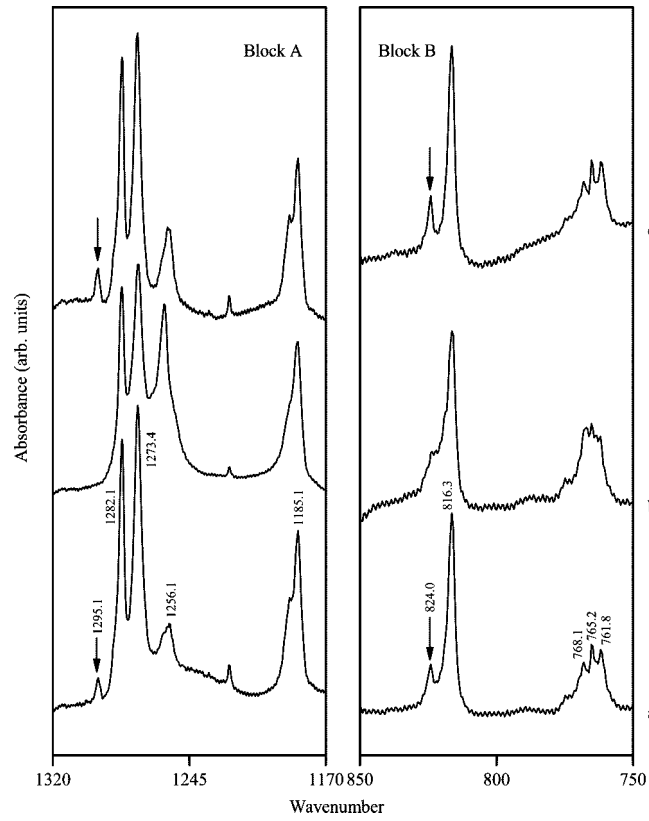

Figure 4. Matrix isolation infrared spectra of as deposited DMHP in nitrogen matrix using different sample deposition technique spanning the region 1320−1170 cm^{-1} (block A) and in the region 850−750 cm^{-1} (block B): (a) an effusive nozzle; (b) supersonic nozzle; (c) an heated effusive nozzle at 373 K.

symmetric and asymmetric stretching, P−H bending and (P−O)−C stretching modes of vibrations in DMHP.[7] Also shown in Figures 1a (blocks A and B) and 2a (block A) is the IR spectrum of liquid DMHP. A comparison of the matrix isolated and the liquid spectra reveals rich and well resolved features obtained when DMHP was trapped in cryogenic matrices. The main spectral features of DMHP in the nitrogen matrix (deposited using a room-temperature effusive source) occur at 549.2, 761.8, 765.2, 768.1, 816.3, 824.0, 976.4, 987.5, 996.6, 1062.7, 1094.0, 1185.1, 1256.1, 1273.4, 1282.1 and 1295.1 cm^{-1}. The spectra in the argon and krypton matrices are very similar, but the peak positions are slightly shifted from the nitrogen matrix values as normally expected in matrix isolation experiments. The relative intensities of some of the features are different in different matrices.

Figure 3a−c shows the matrix isolated spectra when the matrix was annealed at 25 and 30 K in a N_2 matrix. On annealing the matrix at 25 K (Figure 3b) the intensity of the features observed at 1295.1 and 824.0 cm^{-1} slightly decreased whereas on 30 K annealing (Figure 3c) the same features almost vanished completely. Other features observed at 1282.1, 1273.4, 1185.1, 816.3, 768.1, 765.2 and 761.8 cm^{-1} do not show any appreciable change during 25 and 30 K annealing. The features at 1256.1 and 1286.9 cm^{-1} showed an increase in its intensity. Based on our previous work on the phosphate−water[15] system, these features may be due to a phosphonate−water complex in a N_2 matrix. As water is an inevitable impurity in the matrix isolation experiments, we cannot avoid complexes due to water.

We then performed experiments using heated effusive nozzle source. In the heated nozzle experiment the nozzle temperatures were varied over the range 298−435 K. The idea of performing the heated nozzle experiments was to alter the conformational population in the gas phase by heating the sample just prior to deposition. Such an exercise proved fruitful in our earlier experiments with dimethoxymethane (DMM)[16] and diethoxymethane (DEM).[17] The features that increased in intensity when the heated nozzle was used can then be assigned to higher energy conformers.

We also performed experiments using supersonic jet source to look for conformational cooling. DMHP was mixed with N_2 and this gas mixture was expanded through a supersonic nozzle. N_2 served as both the expansion gas and matrix gas, and a stagnation pressure of 1.3 atm was used.

Figure 4a−c compares the "as deposited spectra" of effusive nozzle, supersonic jet and heated nozzle at 373 K experiments of DMHP in nitrogen matrix. From the figure it is clearly evident that the features at 1295.1 and 824.0 cm^{-1} in the "as deposited spectra" of the effusive nozzle experiment vanish in the supersonic jet experiment (Figure 4b) whereas the same features showed an increase in its intensity when the heated nozzle source (373 K) was used (Figure 4c). The experimental observations in the N_2 matrix are

1. No appreciable change in the intensity of features at 1273.4, 1282.1, 1185.1, 816.3, 768.1, 765.2 and 761.8 cm^{-1} noticed in as deposited, supersonic, heating nozzle and annealing experiments.

2. The intensity of 1295.1 and 824.0 cm^{-1} feature vanished in supersonic jet nozzle experiment whereas the same features increased in intensity in the heated nozzle experiment.

3. The intensity of 1295.1 and 824.0 cm^{-1} feature vanished when the matrix was annealed at 30 K.

TABLE 1: Selected Structural Parameters[a] of the Conformers and the Transition States of DMHP Computed at the B3LYP/6-31++G Level**

parameter	$G^{\pm}G^{\mp}$	TS1[b]	$G^{-}G^{-}$	TS2[c]	TG^{+}	TS3[d]	TG^{-}
P1–O2	1.49	1.49	1.49	1.48	1.48	1.48	1.48
P1–H5	1.40	1.41	1.41	1.40	1.41	1.41	1.41
O3–C6	1.45	1.44	1.44	1.44	1.44	1.44	1.44
O4–C7	1.44	1.44	1.44	1.45	1.45	1.44	1.44
C6–H8	1.09	1.09	1.09	1.09	1.09	1.09	1.10
C7–H11	1.10	1.10	1.10	1.10	1.09	1.10	1.10
∠O2–P1–O3	118.6	117.3	117.6	115.1	112.5	116.4	115.1
∠O2–P1–O4	114.5	117.5	117.4	116.1	116.6	116.3	116.6
∠H5–P1–O3	98.5	104.1	103.8	102.2	103.8	103.0	103.8
∠H5–P1–O4	105.1	103.7	104.3	101.0	98.4	104.3	103.2
∠P1–O3–C6	120.5	120.6	119.0	125.4	120.7	126.2	121.6
∠P1–O4–C7	120.4	119.0	120.3	121.3	120.7	120.0	120.1
tor∠O2–P1–O3-C6	51.7	–21.3	–45.9	128.4	–178.6	131.5	177.4
tor∠O2–P1–O4-C7	30.6	47.3	26.4	13.3	–33.1	35.2	38.2
tor∠H5–P1–O3-C6	177.3	104.9	80.0	–105.8	–50.4	–103.9	–56.6
tor∠H5–P1–O4-C7	–97.7	–78.6	–99.7	–138.8	–159.8	–90.3	–88.3
tor∠C6–O3–P1-O4	–75.2	–148.5	–172.9	–0.64	52.8	3.93	50.4
tor∠C7–O4–P1-O3	160.0	174.5	153.6	115.2	93.1	162.8	164.3

[a] Bond lengths in Å and bond angles and dihedral angles in deg. [b] Transition state connecting $G^{\pm}G^{\mp}$ and $G^{-}G^{-}$. [c] Transition state connecting $G^{\pm}G^{\mp}$ and TG^{+}. [d] Transition state connecting $G^{\pm}G^{\mp}$ and TG^{-}.

A similar trend was also observed in argon and krypton matrices. Even though the experiments were performed in nitrogen, argon and krypton matrices, we use nitrogen matrix results for the discussion in this paper. Although we have recorded the spectra over the region 4000−400 cm^{-1}, only the regions 1320−1170 and 850−750 cm^{-1} are shown, as these are the regions that carry information on the conformations of DMHP.

Computational Details. Geometry optimizations were performed at the HF and B3LYP level using 6-31++G** basis set. The optimized structural parameters obtained at the B3LYP/6-31++G** are given in Table 1. The corresponding structures are shown in Figure 5. The structures of different conformers of DMHP differ mainly in the dihedral angle between the O−P−O and P−O−C planes. At B3LYP level four minima corresponding to $G^{\pm}G^{\mp}$, $G^{-}G^{-}$, TG^{+} and TG^{-} conformers[18] in the order of increasing energy were obtained which agreed well with the earlier work by Georgiev et al.[4] Vibrational frequency calculations at B3LYP level yielded all-positive frequencies for the $G^{\pm}G^{\mp}$, $G^{-}G^{-}$, TG^{+} and TG^{-} conformers, confirming that all these structures are minima on the potential energy surface. However at the HF level the $G^{-}G^{-}$ conformer gave one imaginary frequency. Table 2 gives the scaled vibrational frequencies and their mode assignments at B3LYP level for the different conformers. Table 3 gives the raw, zero-point energies (ZPE), relative energies and the dipole moments of the different conformers and the transition states at both the HF and B3LYP levels.

Transition-state calculations were performed at B3LYP/6-31++G** level connecting the ground-state with higher energy conformers. Table 1 gives the structural parameters of the transition states and Figure 5 shows the transition-state structures. Figure 6 shows the plot of relative energies versus the different conformers and the transition state.

Vibrational Assignments. The main spectral features in the N_2 matrix are 549.2, 761.8, 765.2, 768.1, 816.3, 976.4, 987.5, 996.6, 1062.7, 1094.0, 1185.1, 1273.4 and 1282.1 cm^{-1} (marked in Figures 1b and 2b). These features are essentially those of the ground-state conformer, which is indicated by our computations to have a $G^{\pm}G^{\mp}$ structure. The computed, scaled frequencies calculated at B3LYP level fit well with our room-temperature effusive source experiment. Both the experimental and computed frequencies and the mode assignments are given in Table 2. The doublet features at 1273.4 and 1282.1 cm^{-1} behaved similarly on annealing, heating nozzle and supersonic jet experiments. We believe that these features are due to the stable sites of the ground-state conformer. Hence we assign both these features to the P═O stretching mode of the $G^{\pm}G^{\mp}$ conformer.

The first higher energy conformer, $G^{-}G^{-}$, was found to be 1.53 kcal/mol above the ground-state conformer ($G^{\pm}G^{\mp}$). At room temperature the contribution of the $G^{\pm}G^{\mp}$ and $G^{-}G^{-}$ to the overall population is in the ratio 87.9:3.3, computed using the energies and degeneracies shown in Table 3. The contribution of higher energy $G^{-}G^{-}$ conformer to the overall population is very less and the vibrational frequency calculation also revealed that $G^{-}G^{-}$ conformer has a very low barrier (the lowest vibrational frequency ∼8 cm^{-1}) on the potential energy surface. Furthermore, the transition state connecting the $G^{-}G^{-}$ and $G^{\pm}G^{\mp}$ is barrierless (Figure 6). Based on the above reasons, trapping the $G^{-}G^{-}$conformer in the matrix at 15 K is unlikely and hence this conformer is ruled out in our experiments.

The feature observed at 1295.1 and 824.0 cm^{-1} can be assigned to one of the following:

1. Multiple trapping sites.
2. Higher energy conformer (TG^{+} and/or TG^{-}).

Figure 1c,d (block A) and Figure 2c,d (block A) show the "as deposited spectra" of effusive nozzle experiments of DMHP in argon and krypton matrices. From the figure it is clear that in an argon matrix we observed features at 1299.0 and 824.0 cm^{-1} and in krypton matrix at 1303.3 and 840.4 cm^{-1}. These features correspond to 1295.1 and 824.0 cm^{-1} features observed in the "as deposited spectrum" of DMHP in a N_2 matrix. Furthermore, the "as-deposited spectra" obtained in the supersonic jet source experiment showed no intensity for 1295.1 and 824.0 cm^{-1} features (Figure 4b), whereas the same features increased in its intensity in the heated effusive nozzle experiments (373 K) (Figure 4c) compared to the room temperature effusive nozzle experiment (Figure 4a) strongly indicative that these features are indeed due to higher energy conformer and not due to multiple trapping site.

The question now arises as to which of the higher energy conformers (TG^{+} and/or TG^{-}), we can assign the 1295.1 and 824.0 cm^{-1} features. The calculated vibrational frequencies for

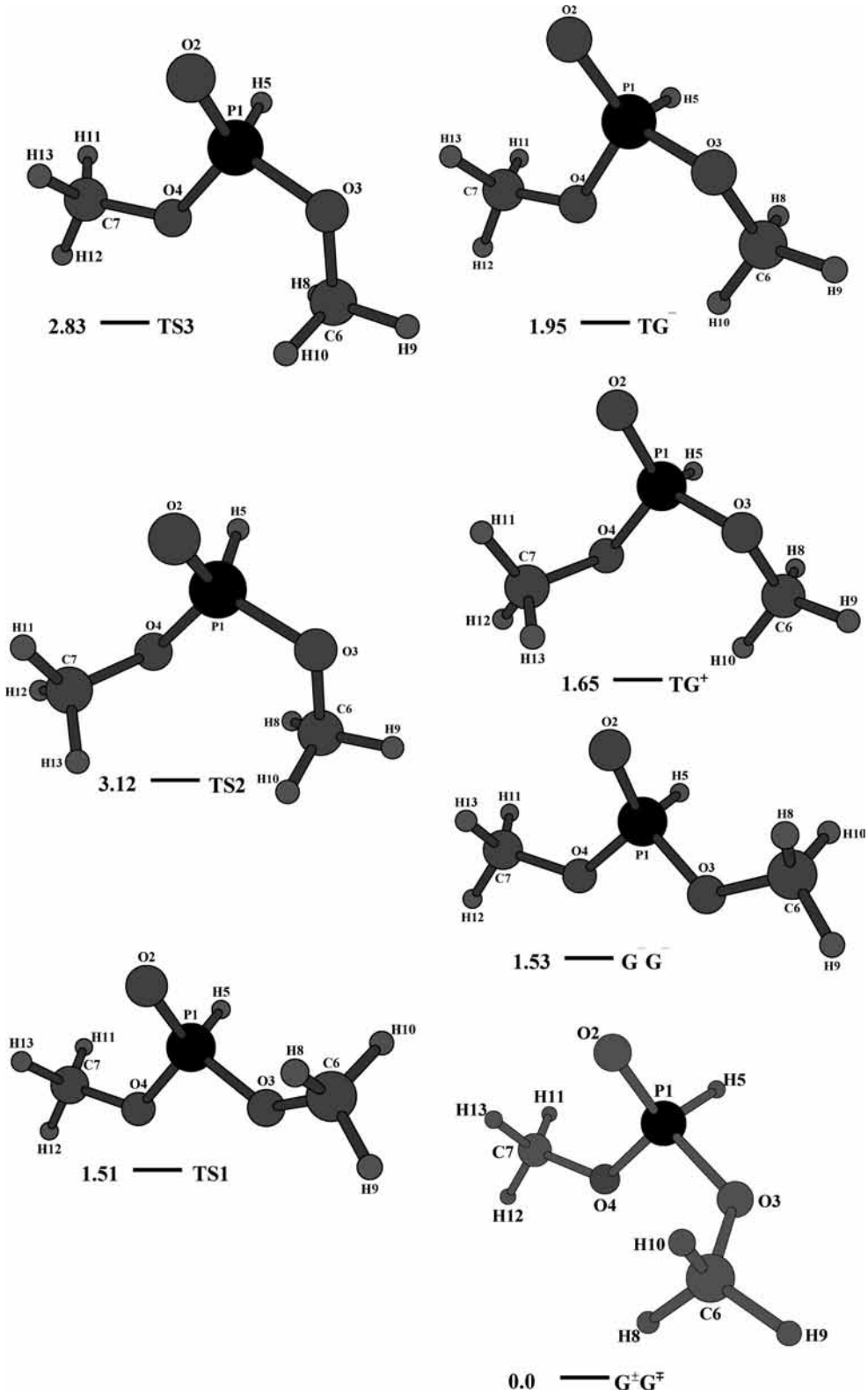

Figure 5. Computed structures of G ± G∓, G⁻G⁻, TG⁺ and TG⁻ conformers. Transition-state structure connecting the ground-state conformer (G ± G∓), and higher energy conformers (G⁻G⁻, TG⁺ and TG⁻) are also shown. Relative energies, in kcal/mol, are given against each structure.

these two conformers TG^+ and TG^- in the P═O stretching region is 1288.5 and 1294.0 cm^{-1} and in the (P−O)−C stretching region is 802.8 and 812.2 cm^{-1}, which are reasonably close to each other. The higher energy conformers TG^+ and TG^- were found to be 1.65 and 1.95 kcal/mol above the $G^{\pm}G^{\mp}$ ground-state conformer. Population calculations using B3LYP energies indicate the contribution of the G ± G∓, G^-G^-, TG^+ and TG^- to the overall population to be in the ratio 87.9:3.3:5.5:3.3. At 373 K the contribution of these conformers to the overall population would be in the ratio 79.8:3.8:12.5:3.9, clearly showing that the TG^+ conformer has a substantial increase in the population when compared with G^-G^- and TG^-. Hence,

TABLE 2: Experimental Vibrational Frequencies in Nitrogen, Argon and Krypton Matrices and Computed Scaled Frequencies[a] of $G^{\pm}G^{\mp}$, $G^{-}G^{-}$, TG^{+} and TG^{-} Conformers of DMHP, Computed at the B3LYP/6-31++G Level (Intensities in Parentheses)**

calculated ν, cm^{-1} $G^{\pm}G^{\mp}$	experimental ν, cm^{-1}			calculated ν, cm^{-1} TG^{+}	experimental ν, cm^{-1}			mode assignments[b]
	N_2	Ar	Kr		N_2	Ar	Kr	
537.3 (44)	549.2	549.2	549.7	536.3 (35)				
745.3 (52)	761.8, 765.2, 768.1	763.8	762.3	736.2 (38)			780.6	$\nu_{(P-O)-C}$ sym.stretching
797.8 (88)	816.3	817.8	815.3	802.8 (153)	824.0	824.0	840.4	$\nu_{(P-O)-C}$ stretching
976.4 (300)	976.4	974.0	973.5	974.3 (216)				ν_{P-H} bending
996.1 (78)	987.5	987.0	981.7	1003.1 (111)				
		991.3	985.6					
			998.1					
1076.2 (255)	1062.7	1066.1	1058.4	1074.9 (185)				$\nu_{P-(O-C)}$ stretching
1112.7 (115)	1094.0	1096.9	1064.6	1095.9 (149)				
			1095.5					
1203.3 (15)	1185.1	1187.6	1185.7	1203.1 (12)				ν_{CH_3} rocking
1206.1 (19)				1204.3 (25)				
1267.3 (222)	1273.4	1274.9	1274.4	1288.5 (253)	1295.1	1299.0	1303.3	$\nu_{P=O}$ stretching
	1282.1	1285.9	1283.5					
2534.6 (80)	2456.5	2446.5	2450.2	2506.8 (82)				ν_{P-H} stretching
3064.3 (54)	2857.0	2856.4	2856.8	3054.2 (44)				ν_{CH_3} sym.stretching
3072.0 (36)				3071.0 (41)				
3146.9 (20)	2963.8	2963.8	2954.5	3130.2 (26)				ν_{CH_3} assym.stretching
3153.4 (16)				3153.3 (19)				
3177.7 (10)	3005.5	3005.5	2996.2	3176.3 (14)				ν_{CH_2} assym.stretching
3181.9 (13)				3181.9 (11)				

calculated ν, cm^{-1}		
$G^{-}G^{-}$	TG^{-}	mode assignments[b]
503.2 (55)	492.3 (42)	
770.1 (87)	753.9 (74)	$\nu_{(P-O)-C}$ sym stretching
808.5 (49)	812.2 (115)	$\nu_{(P-O)-C}$ stretching
982.0 (249)	984.8 (226)	ν_{P-H} bending
1012.2 (31)	1005.7 (27)	
1065.3 (531)	1079.0 (333)	$\nu_{P-(O-C)}$ stretching
1115.5 (24)	1089.2 (95)	
1205.7 (40)	1203.9 (13)	ν_{CH_3} rocking
1207.2 (6)	1207.5 (22)	
1270.1 (205)	1294.0 (265)	$\nu_{P=O}$ stretching
2478.9 (106)	2462.0 (104)	ν_{P-H} stretching
3058.5 (53)	3056.6 (44)	
3067.8 (47)	3062.8 (48)	ν_{CH_3} sym.stretching
3141.1 (20)	3140.3 (23)	
3151.1 (20)	3146.9 (20)	ν_{CH_3} assym.stretching
3181.5 (11)	3180.7 (15)	
3182.7 (11)	3181.0 (8)	ν_{CH_2} assym.stretching

[a] Scaling factor used was 1.005. [b] Mode assignments based on ref 7 and vibrational visualization program Gauss View 2.1.

the features observed at 1295.1 and 824.0 cm^{-1} are assigned to the higher energy conformer TG^{+}. Calculations indicated that this conformer has a dipole moment 4.29 D.

Annealing Experiments. Figure 3 shows the annealing of DMHP in N_2 matrix at different temperatures. On annealing DMHP at 25 K (Figure 3b) the intensity of the 1295.1 and 824.0 cm^{-1} features decreases and at 30 K these features completely vanished (Figure 3c). This observation could be due to

1. Conformer interconversion in the matrix $TG^{+} \rightarrow G^{\pm}G^{\mp}$.
2. Aggregation/association of impurities such as water with phosphonate.

Conformer interconversion in matrix is possible by annealing the matrix, which depends upon the energy barrier for the internal rotation as pointed by Barnes.[19] A rough estimate of these energy barriers can be made by determining the temperature at which the processes start to occur. On annealing the matrix, conformational interconversion was observed for alcohols such as methanol and ethanol isolated in different matrices.[20,21] In these molecules the gas-phase energy barriers are less than 1.43 kcal/mol. Reva et al.[22,23] observed gauche to cis conformer interconversion for methyl cyanoacetate (MCA) at 40K and cyanoacetic acid (CAA) at 20K in xenon matrices. Ab initio calculations predicted that both these molecules have isoenergetic conformers separated by low energy barriers 0.71 kcal/mol. Stepanian et al.[24,25] observed three conformers for the glycine molecule in an argon matrix as predicted by ab initio and density functional calculations. On annealing the matrix above 13 K they observed interconversion of conformer III to conformer I.

In the case of DMHP the predicted gas-phase energy barrier for $TG^{+} \rightarrow G^{\pm}G^{\mp}$ is 1.47 kcal/mol (Figure 6). Hence, we can expect conformer interconversion to take place in our annealing experiments. The annealing experiments clearly show (Figure 3) the intensity of the higher energy conformer frequencies (1295.1 and 824.0 cm^{-1}) vanish at 30 K. It has been reported that matrix affects the relative energies of the conformers and energy barriers for conformational interconversion when compared with values of the individual molecules in the gaseous phase.[26–29] It is also observed that the conformer with a higher dipole moment is stabilized more in the polar matrix [30,31] In

TABLE 3: Raw Energy/ZPE Corrected Energy, Relative Energy and the Dipole Moment (D) of the $G^{\pm}G^{\mp}$, $G^{-}G^{-}$, TG^{+}, and TG^{-} Conformers and the Transition States of DMHP at B3LYP and HF Using the 6-31++G Basis Set**

		energy (hartrees)				relative Energy[d]		dipole moment (D)[e]	
conformer	degeneracy	B3LYP[a]	B3LYP[b]	HF[a]	HF[c]	B3LYP	HF	B3LYP	HF
$G^{\pm}G^{\mp}$	2	−647.51453	−647.41376	−645.19006	−645.09336	0	0	2.40	2.64
$G^{-}G^{-}$	1	−647.51175	−647.41133	−645.18754	−645.09126	1.53	1.32	1.68	1.75
TG^{+}	2	−647.51180	−647.41114	−645.18690	−645.09029	1.65	1.93	4.29	4.72
TG^{-}	2	−647.51121	−647.41066	−645.18640	−645.08988	1.95	2.18	4.54	4.87
TS1[e]		−647.51175	−647.41136			1.51		1.62	
TS2[f]		−647.50902	−647.40878			3.12		4.12	
TS3[g]		−647.50962	−647.40926			2.83		4.25	

[a] Raw energy. [b] ZPE corrected energy (scaling factor 1.005). [c] ZPE corrected energy (scaling factor 0.8949). [d] Relative energy in kcal/mole. [e] Dipole moment in Debye units. [f] Transition state connecting $G^{\pm}G^{\mp}$ and $G^{-}G^{-}$. [g] Transition state connecting $G^{\pm}G^{\mp}$ and TG^{+}. [h] Transition state connecting $G^{\pm}G^{\mp}$ and TG^{-}.

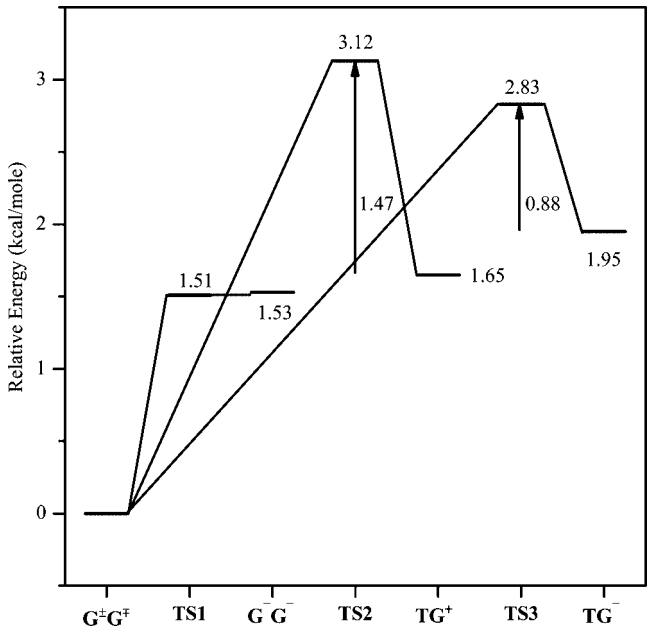

Figure 6. Plot showing the relative energies in kcal/mol of different conformers and the transition states connecting the ground-state conformer ($G^{\pm}G^{\mp}$) and higher energy conformers ($G^{-}G^{-}$, TG^{+} and TG^{-}).

the case of DMHP, we observed the higher energy conformer TG^{+}, which has a higher dipole moment 4.29 D, has a higher intensity in more polarizable krypton matrix (Figure 1d). Unlike in the case nitrogen and argon matrices the intensity of the higher energy conformer in krypton matrix (1303.3 and 840.4 cm^{-1}) did not vanish completely on annealing.

A decrease in intensity of the infrared feature in the matrix on annealing can also be due to aggregation and/or adduct formation. In our experiment we have observed adduct features of DMHP with water at 1256.1 and 1286.9 cm^{-1}. These adduct features are also observed in argon and krypton annealing experiments. Hence, we believe that both conformational interconversion and DMHP−water adduct formation compete with each other in our experiments.

5. Conclusion

Conformations of DMHP isolated in nitrogen, argon and krypton matrices were studied for the first time. DFT calculations predicted four stable conformers $G^{\pm}G^{\mp}$, $G^{-}G^{-}$, TG^{+} and TG^{-} in the order of increasing energy and the vibrational frequency calculations predicted all the four conformers are indeed a minimum on the potential energy surface Experiments and calculation resulted in assigning the vibrational frequencies for the ground-state $G^{\pm}G^{\mp}$ and higher energy TG^{+} conformers of DMHP. Transition-state calculation and the energy barriers were obtained for the conformer interconversion. The energy barrier for conformer interconversion between $G^{-}G^{-} \rightarrow G^{\pm}G^{\mp}$ is barrierless whereas for the $TG^{+} \rightarrow G^{\pm}G^{\mp}$ it is 1.47 kcal/mol and for $TG^{-} \rightarrow G^{\pm}G^{\mp}$ it is 0.88 kcal/mol. Both conformational interconversion and adduct formation are observed on annealing the matrix.

Acknowledgment. We thank CVS Brahmananda Rao, IGCAR, Kalpakkam, for helping us in preparing and characterizing the Dimethylhydrogen phosphonate (DMHP) sample.

References and Notes

(1) Toy, A. D.; Walsh, E. N. *Phosphorus Compounds in Everyday Living*; American Chemical Society: Washington, DC, 1987.

(2) *The Pesticide Manual*, 9th ed.; Worthing, C. R., Hance, R. J. Eds.; British Crop Protection Council: Surrey, U.K., 1991.

(3) Van Wazer, J. R.; Ewig, C. S. *J. Am. Chem. Soc.* **1986**, *108*, 4354.

(4) Georgiev, E. M.; Kaneti, J.; Troev, K.; Roundhill, D. M. *J. Am. Chem. Soc.* **1993**, *115*, 10964.

(5) Barnes, A. J.; Lomax, S.; Van der Veken, B. J. *J. Mol. Struct.* **1983**, *99*, 137.

(6) Vishnyakov, A.; Neimark, A. V. *J. Phys. Chem. A* **2004**, *108*, 1435.

(7) Katcyuba, S. A.; Monakhova, N. I.; Ashrafullina, L. Kh.; Shagidullin, R. R. *J. Mol. Struct.* **1992**, *269*, 1.

(8) Pieters, G. H.; Van Der Veken, B. J.; Barnes, A. J.; Little, T. S.; Durig, J. R. *J. Mol. Struct.* **1984**, *125*, 243.

(9) Vidya, V.; Sankaran, K.; Viswanathan, K. S. *Chem. Phys. Lett.* **1996**, *258*, 113.

(10) George, L.; Viswanathan, K. S.; Singh, S. *J. Phys. Chem.* **1997**, *101*, 2459.

(11) Sankaran, K.; Venkatesan, V.; Sundararajan, K.; Viswanathan, K. S. *J. Indian Inst. Sci.* **2005**, *85*, 403.

(12) George, L.; Sankaran, K.; Viswanathan, K. S.; Mathews, C. K. *Appl. Spectrosc.* **1994**, *48*, 7.

(13) Coulson, E. J.; Gerrard, W.; Hudson, H. R. *J. Chem. Soc.* **1965**, 2364.

(14) Frisch, M. J.; Trucks, G. W.; Schlegel, H. B.; Gill, P. M. W.; Johnson, B. G.; Robb, M. A.; Cheeseman, J. R.; Keith, T.; Petersson, G. A.; Montgomery, J. A.; Raghavachari, K.; Al-Laham, M. A.; Zakrzewski, V. G.; Ortiz, J. V.; Foresman, J. B.; Cioslowski, J.; Stefanov, B. B.; Nanayakkara, A.; Challacombe, M.; Peng, C. Y.; Ayala, P. Y.; Chen, W.; Wong, M. W.; Andres, J. L.; Replogle, E. S.; Gomperts, R.; Martin, R. L.; Fox, D. J.; Binkley, J. S.; Defrees, D. J.; Baker, J.; Stewart, J. J. P.; Head-Gordon, M.; Gonzalez, C.; Pople, J. A. *Gaussian 94*, revision B.3; Gaussian, Inc.: Pittsburgh, PA, 1995.

(15) Sankaran, K.; Vidya, V.; Viswanathan, K. S.; George, L.; Singh, S. *J. Phys. Chem.* **1998**, *102*, 2944.

(16) Venkatesan, V.; Sundararajan, K.; Sankaran, K.; Viswanathan, K. S. *Spectrochim. Acta Part A* **2002**, *58*, 467.

(17) Venkatesan, V.; Sundararajan, K.; Viswanathan, K. S. *J. Phys. Chem A* **2003**, *107*, 7727.

(18) The notations "G and T" refers to a gauche and trans orientation of the carbon atoms, C6 and C7 carbons with respect to O2; for example, the dihedral angle between planes O2P1O3 and C6O3P1 and in the ground-state conformer is 51.7° and hence is referred to as gauche. The plus sign

refers to the orientation of the $-CH_3$ group away from the hydrogen H5 and the minus sign toward the hydrogen H5 in the OPO plane.

(19) Barnes, A. J. *J. Mol. Struct.* **1984**, *113*, 161.

(20) Serrallach, A.; Meyer, R. *J. Mol. Spectrosc.* **1976**, *60*, 246.

(21) Barnes, A. J.; Whittle, G. C. *Proc. Eur. Congr. Mol. Spectrosc., 12th* **1976**, 373.

(22) Reva, I. D.; Ilieva, V. S.; Fausto, R. *Phys. Chem. Chem. Phys.* **2001**, *3*, 4235.

(23) Reva, I. D.; Stepanian, S. G.; Adamowicz, L.; Fausto, R. *Chem. Phys. Lett.* **2003**, *374*, 631.

(24) Stepanian, S. G.; Reva, I. D.; Radchenko, E. D.; Rosado, M. T. S.; Duarte, M. L. T. S.; Fausto, R.; Adamowicz, L. *J. Phys. Chem. A* **1998**, *102*, 1041.

(25) Reva, I. D.; Plokhotnichenko, A. M.; Stepanian, S. G.; Ivanov, A.Yu.; Radchenko, E. D.; Sheina, G. G.; Blagoi, Y. P. *Chem. Phys. Lett.* **1995**, *232*, 141.

(26) Molnár, F.; Dick., B. *Ber. Bunsen-Ges. Phys. Chem.* **1995**, *99*, 422.

(27) Fraenkel, R.; Haas, Y. *Chem. Phys.* **1994**, *186*, 185.

(28) Fraenkel, R.; Kahana, S.; Haas, Y. *Ber. Bunsen-Ges. Phys. Chem.* **1995**, *99*, 412.

(29) Eriksson, L. A.; Laaksonen, A. *J. Chem. Phys.* **1996**, *105*, 8195.

(30) Kulbida, A.; Ramos, M. N.; Räsänen, M.; Nieminen, J.; Schrems, O.; Fausto, R. *J. Chem. Soc., Faraday Trans.* **1995**, *91*, 1571.

(31) Fausto, R.; Kulbida, A.; Schrems, O. *J. Chem. Soc., Faraday Trans.* **1995**, *91*, 3755.

JP800604Y